

## CHANGES IN OPTICAL PROPERTIES AS SENSITIVE AND REPRODUCIBLE CHARACTERISTICS OF FUSION PHENOMENA\*

H. P. VAUGHAN

*Mettler Instrument Corporation, Princeton, New Jersey 08540 (U. S. A.)*

(Received September 15th, 1969)

### ABSTRACT

Many temperature dependent physical and chemical changes also involve changes in the optical properties of the sample; *i.e.*, changes in the amount or color or polarization of light reflected from or transmitted through the sample. When an accurately measured temperature is changed in a prescribed manner, a very precise determination of the occurrence of a phenomenon can be made since the visual changes are often very large.

Applications of a new apparatus for precise thermometry based on this method are shown. Organic and polymer fusion phenomena are described.

### INTRODUCTION AND DISCUSSION

Many temperature dependent physical and chemical changes also involve changes in the optical properties of the sample; *i.e.*, changes in the amount or color

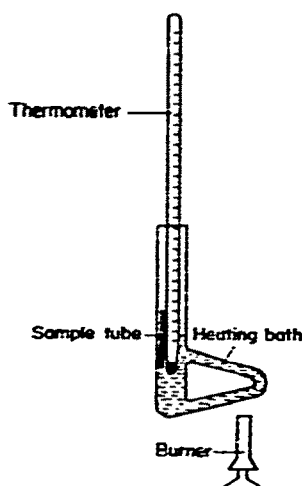


Fig. 1a. The capillary melting-point apparatus of Thiele.

\*Presented at the Recent Advances in Thermal Analysis Symposium, American Chemical Society Meeting, Houston, Texas, U.S.A., February 22-27, 1970.

or the polarization of light reflected from or transmitted through the sample. Although such observation gives little or no information regarding possible mass changes or

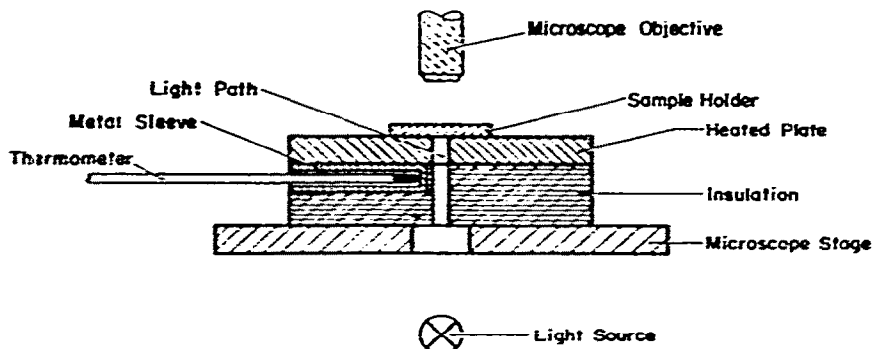


Fig. 1b. The electrically heated microscope hot stage of Kofler.

the energy involved in a transformation or reaction, very precise determination of the occurrence of a phenomenon can be made since the visual changes are often very large. Samples as small as 2–3 mg can be observed with the unaided eye, and samples smaller than a microgram can be observed with a simple microscope. When the temperature of the sample is changed in a prescribed manner, precise observations of the phenomenon and the temperature at which it occurs can be made. The capillary melting-point apparatus of Thiele and the microscope hot stage of Kofler were both based on this measurement principle<sup>1, 2</sup> (Fig. 1).

The most important applications for this technique have been in measurement of melting points and ranges used for identification of materials, level of purity measurement and construction of phase diagrams. Many other useful applications have been found, such as studies of crystal growth, polymorphism, decomposition and evidence of chemical reaction with other compounds, particularly in the case of the hot stage microscope<sup>3</sup>.

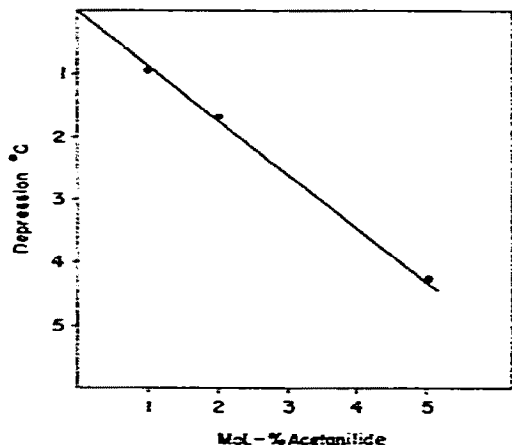


Fig. 2. The melting-point depression of benzoic acid with known amounts of acetanilide as the added impurity.

The ultimate usefulness of any of these applications, however, depends largely on how precisely a phenomenon such as melting can be observed and how accurately the corresponding temperature can be measured. Detection of small changes in purity,<sup>5</sup> or precise molecular weight determination procedures by the Rast method<sup>6</sup> may involve temperature differences in the melting point of only a few tenths of a degree. This can be readily seen in Fig. 2 which shows the relationship between melting-point depression and mole-percent impurity of benzoic acid with acetanilid as the measured impurity.

The relationship, which can be applied to impurities not soluble in the solid phase, is based on a knowledge of the cryoscopic constant,  $\Delta H_f/RT_o^2$ . The relationship is expressed as:

$$\text{Mole \% impurity} = 100 (\Delta H_f/RT_o^2) \Delta T$$

where:

$\Delta H_f$  = heat of fusion of the pure substance, cal/mole

$R$  = the gas constant, cal/deg.mole

$T_o$  = the melting point of the pure substance

$\Delta T$  = the temperature difference between the final melting point of the impure sample and  $T_o$

The cryoscopic constant of many organic substances lies between 0.75 and 2, which means that the melting-point depression ( $\Delta T$ ) would be, on the average, between approx. 1.3 and 0.5°C per mole percent impurity.

## EXPERIMENTAL

### *Measurement of temperature*

Temperature measurement of very small samples presents some difficult problems, particularly if the temperature is being dynamically changed as is the case with most melting-point procedures. In an ideal case (Fig. 3, dashed line), the temperature of a pure substance rises along with the temperature of the heating bath or furnace until it reaches the melting point. At the melting point the bath temperature continues to rise while the temperature of the sample remains constant for a length of time sufficient for the sample to absorb energy equal to the heat of fusion. The temperature of the now liquid sample then rises rapidly and continues to follow the bath temperature.

It is not possible, however, to measure the actual sample temperature but only the temperature of some measuring element (thermometer bulb, thermocouple or resistance thermometer) placed close to, or in contact with, the sample. Even in the best of cases, a layer of liquid melt will separate the temperature element from the remaining solid sample. Any attempt to measure the actual melt isotherm of a small sample, will result in the *measured* temperature differing from the true sample temperature, the extent of which depends on (a) the total heat capacity of the temperature

element compared to the sample, (b) thermal conductivity of the element (conduction along the thermocouple wires or up the stem of a thermometer, *etc.*), (c) the degree of contact between the sample and the element<sup>7</sup>. The solid line in Fig. 3 shows the resulting actual temperature measurement of sample of *p*-nitrotoluene melted in a 2.3-mm capillary with a thermocouple imbedded in the center of the sample.

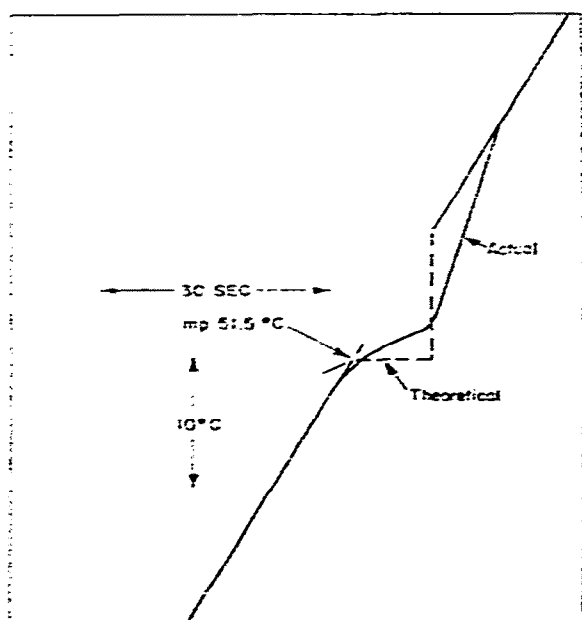


Fig. 3. Heating curve of *p*-nitrotoluene measured by imbedding a thermocouple in the sample. The dashed line shows the actual measured temperature of the thermocouple junction.

The true melt isotherm cannot be measured accurately unless the mass of the sample is very large in comparison to the mass of the temperature element and the mass of the remaining solid sample is large compared to the mass of the melt. This condition is achieved with the very accurate, isothermal NBS triple point cell method, but 100–400 g of material is normally used<sup>8, 9</sup>, making it impractical for routine tests.

The common solution to the problem of measurement of the temperature of small samples has been to place both the sample and the temperature measuring element in a common oil or air bath. In a well designed system, the sample temperature and measuring element temperature will be equal (at moderate rates of heating), except during the occurrence of enthalpic phenomenon such as endothermic melting. The difference between the true sample temperature and the bath temperature during melting, for example, will be a function of the heating rate and time required for melting.

Fig. 4 shows that there is an approximately linear relationship between the apparent melting range (the bath temperature interval between the beginning of melting and the disappearance of the last crystal) and the square root of the heating rate. If a pure substance which melts isothermally is assumed, then the temperature

difference between the solid sample and bath,  $\Delta T$ , at any time during melting,  $t_x$ , would be equal to  $(t_x - t_0)(\Delta T/\Delta t)$  where  $t_0$  is the time of the beginning of melting and  $\Delta T/\Delta t$ , the heating rate.  $\Delta T$  is also the melting range, so that the time required for melting at a given heating rate depends on the rate of heat flow from the heating source, the mass of the sample, its heat of fusion, and the thermal conductivity and specific heat of the liquid melt around the remaining crystals — or the sum total of factors affecting the rate of heat flow and the amount of heat required to melt the

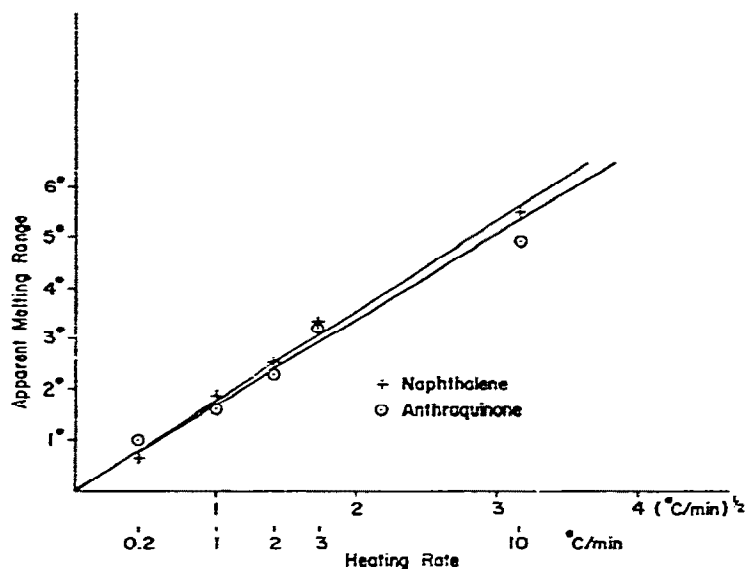


Fig. 4. The apparent melting range (indicated bath temperature) from the beginning of melting to the melting of the last crystal is shown to be proportional to the square root of the heating rate.

sample. All other things being constant, variations in heating rate alone will cause substantial variation in the *apparent* melting range and in the *apparent* melting point of the last crystal. Impurities in the sample will form lower melting-point mixtures, which will cause a *real* increase in the melting range as well as a lowering of the melting point of the last crystal (Fig. 9). Small levels of impurity cannot easily be detected, therefore, unless the heating rate (and, consequently, the apparent melting range) is under very strict control.

Thus, it is obvious that control of the rate of heating is as important to accurate measurements as the absolute accuracy of the temperature measuring element. Accurate control of heating rate was rarely realized with previous types of melting-point apparatus, where heating-rate control was achieved through manual control of an autotransformer or Bunsen burner. Regardless of the type of detection system, a prerequisite for accurate measurements is a linear and reproducible heating rate which can best be achieved through a carefully designed automatic temperature control system.

Fig. 5 shows a schematic of the temperature measurement and control system used with the Mettler capillary and thermal microscopy melting apparatus which were used in all the examples shown. Temperature is measured with a platinum

resistance element placed in very close proximity to the sample holder. Power to the heating elements is proportionally controlled by the difference between the resistance of the temperature element and the resistance of a motor driven potentiometer. The potentiometer resistance curve has been matched to the platinum sensor resistance curve by a shaping network. As long as the actual temperature and required program

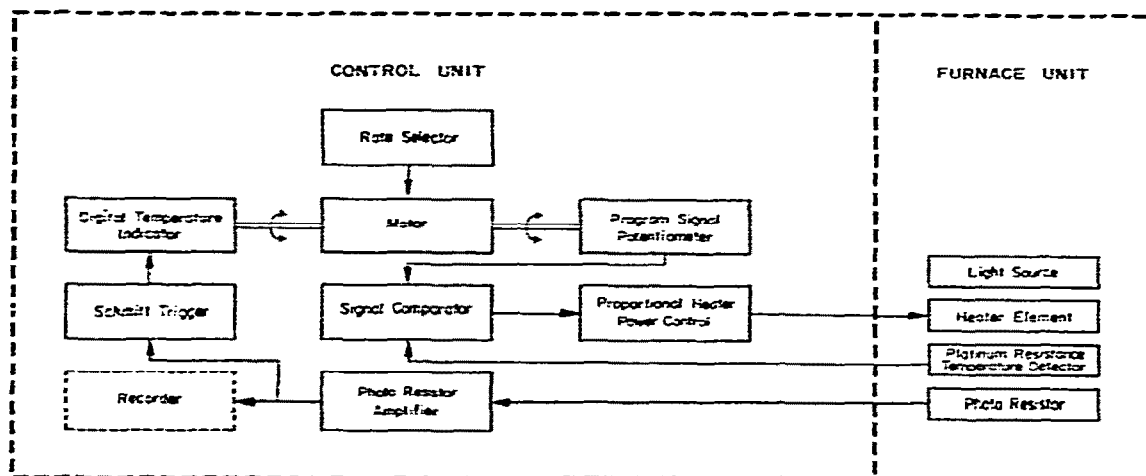


Fig. 5. Schematic control system of the Mettler FP-1 and FP-2 capillary and microscope melting-point instruments.

temperature are in agreement, the rotation of the program signal generator motor will be in linear function of temperature. In this way, it is possible to give a digital temperature presentation by connecting the linear program signal motor to a series of counter wheels. Resulting temperature measurement and control accuracy is  $\pm 0.1^\circ\text{C}$  below  $100^\circ\text{C}$  and  $\pm 0.1\%$  above  $100^\circ\text{C}$ . Program motor speeds corresponding to heating rates between  $0.2$  and  $10^\circ/\text{min}$  are selected in definite steps, thus assuring reproducibility of the program rate.

#### *Observation and measurement of change in light transmission*

Although phenomena involving changes in light transmission or color can be observed directly, the human eye is subjective and results may differ widely from observer to observer. Constant visual observation of the sample can also be very tedious, especially when slow rates of heating and long observation times are required. Electronic observation by means of a photoresistor, amplifier and recorder combination provide an objective and automatic means of obtaining reproducible data which is continuous throughout the temperature range of interest. Two systems suitable for detection of light-transmission changes in a capillary sample holder and on a microscope slide are shown in Figs. 6 and 7.

#### *Capillary measurements*

In the capillary system shown in Fig. 6, the locations of the capillary, light source, and photoresistor are fixed. Powdered samples are normally packed to a

height of 3–4 mm in the bottom of a disposable glass capillary. Fats, oils or waxes can also be easily loaded into the capillary in their melted state by means of a long syringe and then allowed to solidify. The fixed location of the sample and constant light source give results which are easily reproduced without readjustments to the system

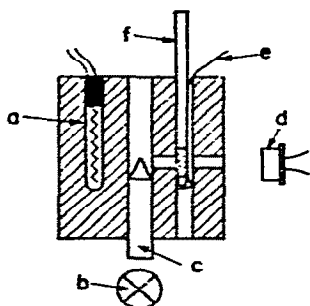


Fig. 6. Schematic figure of the heating block of the capillary melting-point unit: a) aluminium heating block, b) light source, c) glass rod light pipe, d) photoresistor, e) leaf spring capillary tube support, f) capillary tube sample holder (1.2 mm diameter). A platinum resistance element is imbedded in the heating block symmetrically located with respect to the capillary sample holder.

or to the recorder. Fig. 8 shows the excellent agreement of results obtained by the melting of ten different samples of anthraquinone recorded at  $0.2^\circ/\text{min}$ . The total signal change on the recorder is approximately 80 mV. As the substance goes through the melting process in the capillary tube, the yet unmelted crystals move or rotate in the liquid melt. The photoresistor detects this movement and records it as random

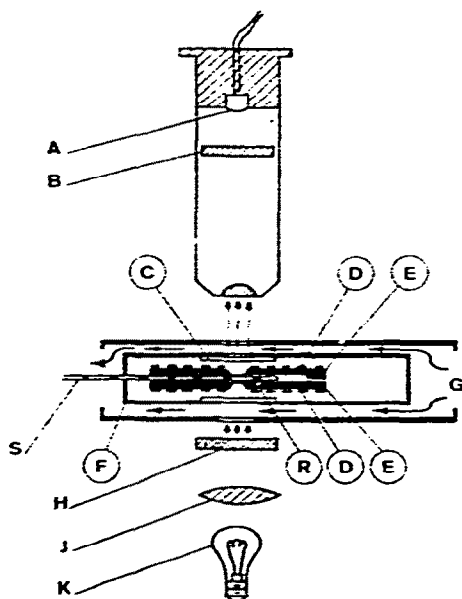


Fig. 7. Microscope hot stage, showing a photoresistor used in place of the normal microscope eyepiece; A) photoresistor, B) polarizing filter, C) heat filter, D) heating elements, E) upper and lower heating platens, F) metal enclosure, G) cooling gas flow, H) polarizing filter, J) condenser lens, K) light source, R) platinum resistance-temperature detector, S) sample carrier slide.

jumps on the recording curve which can be clearly seen in the figure. These small jumps are usually of no significance when recording curves of pure materials. Fig. 9, on the other hand, shows a curve with a broad shoulder which in this case is the effect

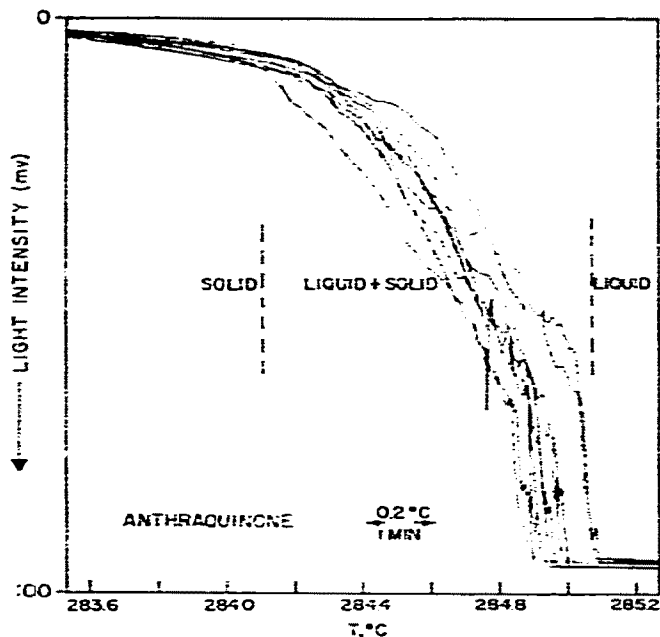


Fig. 8. Photograph of the recording of the photometric curves of ten different samples of anthraquinone (Fisher "Thermetric" Standard T.P. 284.23°C) heated in a capillary tube at 0.2°/min. The recorder chart was returned each time to the same beginning point, so that all curves could be recorded on the same section of chart; 80% of the values fall within  $\pm 0.075^\circ\text{C}$ .

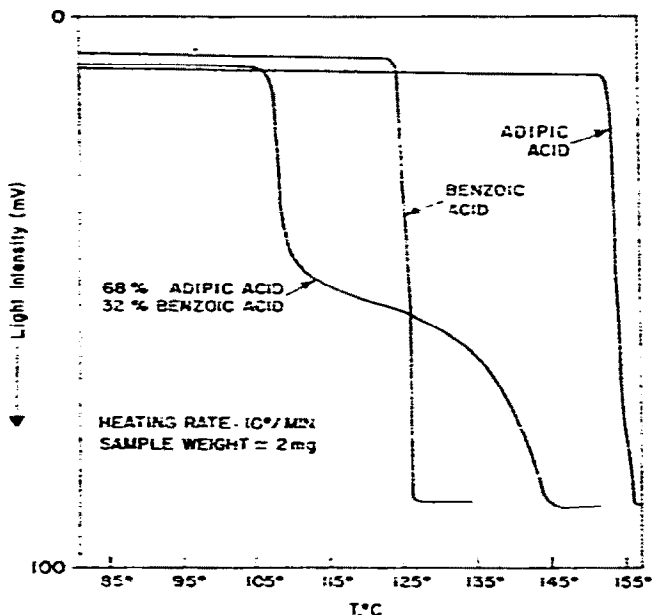


Fig. 9. Photometric curves of the capillary melting of adipic acid, benzoic acid, and a mixture of the two. The adipic-benzoic acid eutectic melting can be seen at 105°C followed by the gradual melting of excess adipic acid up to 145°C.



of a large impurity — 32% benzoic acid in adipic acid. Eutectic melting can be seen at about 105°C followed by the melting of excess adipic acid until about 145°C. Fig. 10 shows the melting and decomposition behavior of refined and raw sugar. The decomposition of the refined sugar takes place over a very narrow range just above 200°C, whereas the raw sugar shows decomposition beginning just after melting. Decomposition is detected by the photoresistor by either detecting a change in color of the clear melt—usually to brown or black—or by detecting the formation of a large gas bubble which pushes the sample out of the path of the light beam.

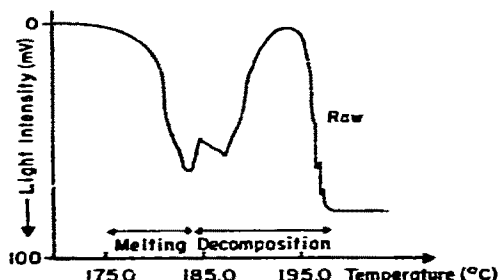
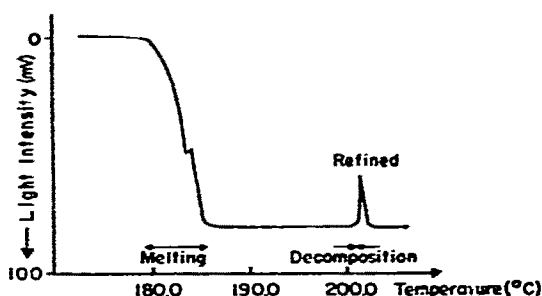


Fig. 10. The melting and decomposition of refined sugar (above) and raw sugar (below). Decomposition of the refined sugar is denoted by the spike at 200°C. Decomposition of the raw sugar takes place over a much broader range.

The examples shown so far have been with materials which change from essentially opaque white solids to clear liquids. The total signal change of colored substances depends on the color. The color response of the CdS photoresistor used<sup>10</sup> is given in Fig. 11, showing the weakest response to be in the blue region. Fig. 12 shows the melting of azulene, which is a dark blue liquid when melted. Even though the signal is reduced, the melting behavior is clearly evident. Even with substances transmitting a nearly full color spectrum, cases occur in which the total change in transmission is very small. Fig. 13 shows an example of the melting of a 2–3% dispersion of paraffin crystals in otherwise clear fuel oil, in which the signal change is only about 10% of that of an opaque substance but still a reliable indicator of the melting phenomenon.

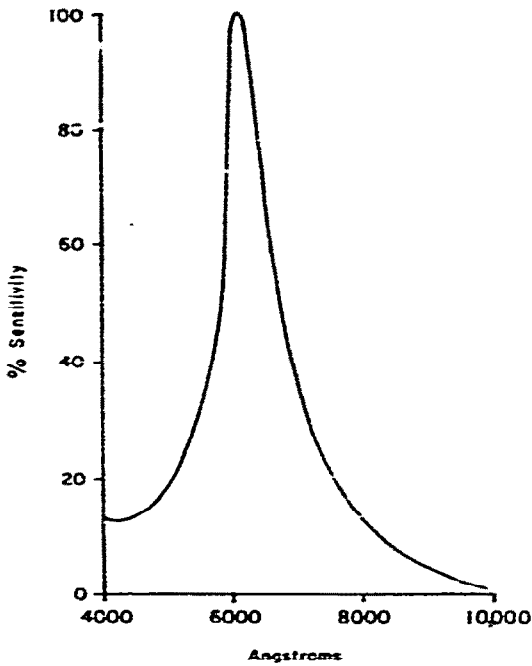


Fig. 11. Spectral response of the CdS photoresistor used in both types of melting apparatus.

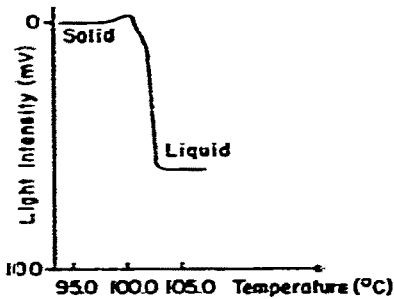


Fig. 12. Photometric curve of the capillary melting of dark blue azulene. Photoresistor signal change is reduced to about 2/3 of the normal signal change (80 mV).

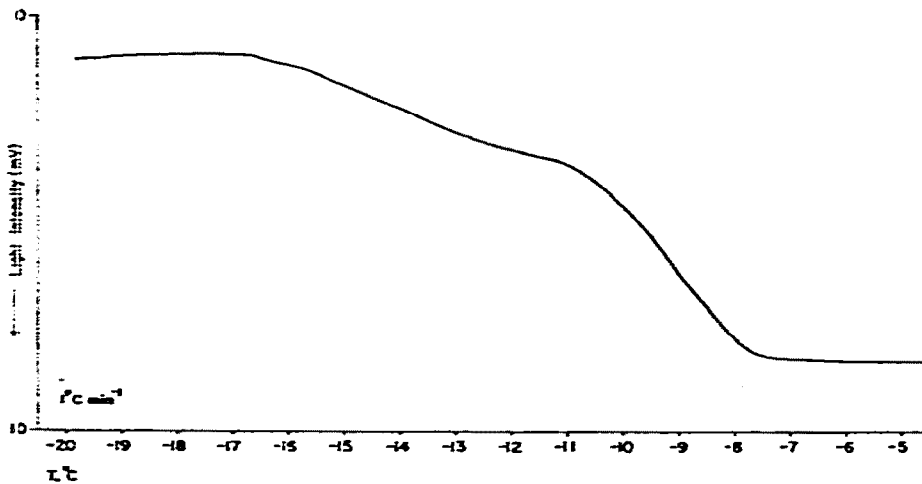


Fig. 13. The melting of a 2-3% paraffin cloud in clear fuel oil. The total signal change is only about 10% of the normal signal change for an opaque substance.

The melting ranges of relatively pure substances ( $\geq 95\%$ ) are comparatively small and their resulting melting curves are sharp. In these cases it is possible to evaluate a characteristic melting temperature digitally without the use of a recorder. If a voltage sensitive switching device (in this case, a variation of the classic Schmitt Trigger) is preset to switch at a specified voltage value corresponding approximately to a point at which the melting process is two thirds complete, this switch closure can be used to lock a digital counter which until this time has shown the value as the digital program temperature indication. This value was chosen by test as the most reproducible value on the melting curve and the one which, by taking into consideration the effect of heating rate on the apparent melting range (Fig. 4), best approximates at slow rates of heating (*e.g.*,  $0.2^\circ/\text{min}$ ) the equilibrium melting temperature. The accuracy and reproducibility of this indication method has been shown to be better than  $0.1^\circ\text{C}$  when compared to the isothermal triple-point technique with such standard pure substances as benzoic acid<sup>11</sup>.

Table I shows the use of this digital indication technique in the evaluation of the progressive purification by crystallization of a preparation of azobenzene. All measurements were made at a heating rate of  $0.2^\circ/\text{min}$ .

TABLE I  
PURIFICATION OF AZOBENZENE

	<i>M.p.</i> <sup>a</sup> ( $^\circ\text{C}$ )	$\sigma_1$ ( $^\circ\text{C}$ )
Original preparation	67.08	$\pm 0.14$
1st Crystallization	67.79	$\pm 0.08$
2nd Crystallization	68.10	$\pm 0.10$
3rd Crystallization	68.18	$\pm 0.10$
4th Crystallization	68.21	$\pm 0.08$

<sup>a</sup>Mean value of nine separate measurements; individual measurements are read to the nearest  $0.1^\circ\text{C}$  only.

### *Thermal microscopy*

Photometric measurement of samples on a microscope hot-stage presents a problem only in that the amount of light being measured depends on the type of light source being used, magnification, size of the sample, *etc.*, in relation to the field of view. Polarized light is normally used with anisotropic substances to increase viewing contrast. Most crystalline organic substances, for example, appear brightly colored under polarized light, while the amorphous glass slide and liquid melt appear as a dark field. Considerable variation in color and in light intensity may be found under polarized light even with the same material due to differences in orientation of the crystal, crystal size and thickness of the sample layer. Best viewing (and recording) conditions are achieved when the sample has been previously melted and then slowly recrystallized between the slide and a cover slip. Polymer films and fibers, however, must usually be measured without premelting because the additional thermal treat-

ment may cause structural changes and will, in any event, eliminate the chance of observing characteristic changes in birefringence of highly crystalline drawn films and fibers normally seen beginning 50 to 60°C below the final melt temperature (Fig. 14).

Fig. 15 shows simultaneous photomicrographs and photometric recording of the growth and melting of a single crystal of vanillin. The crystal was grown by first melting about 0.5 mg of vanillin under a cover slip in the hot stage, freezing it quickly

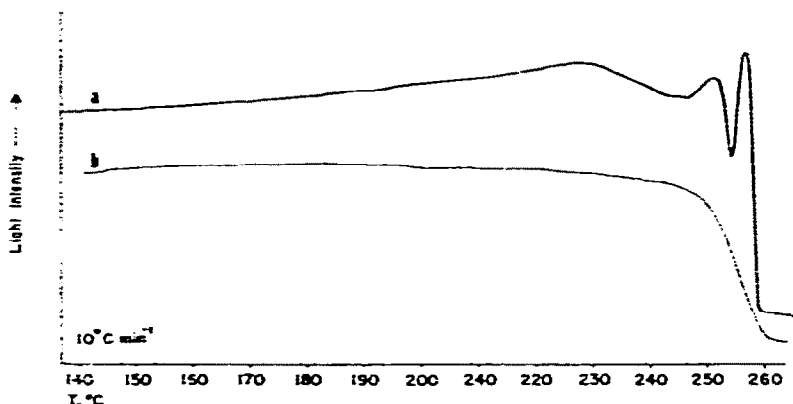


Fig. 14. The melting of Mylar\* film on the microscope hot stage. a) Initial melting showing bright birefringence color changes, b) second melting after recrystallization showing only a change from grey-white to black at 260°C. Color changes during the initial melting are presumably due to stress imparted during the drawing of the film.

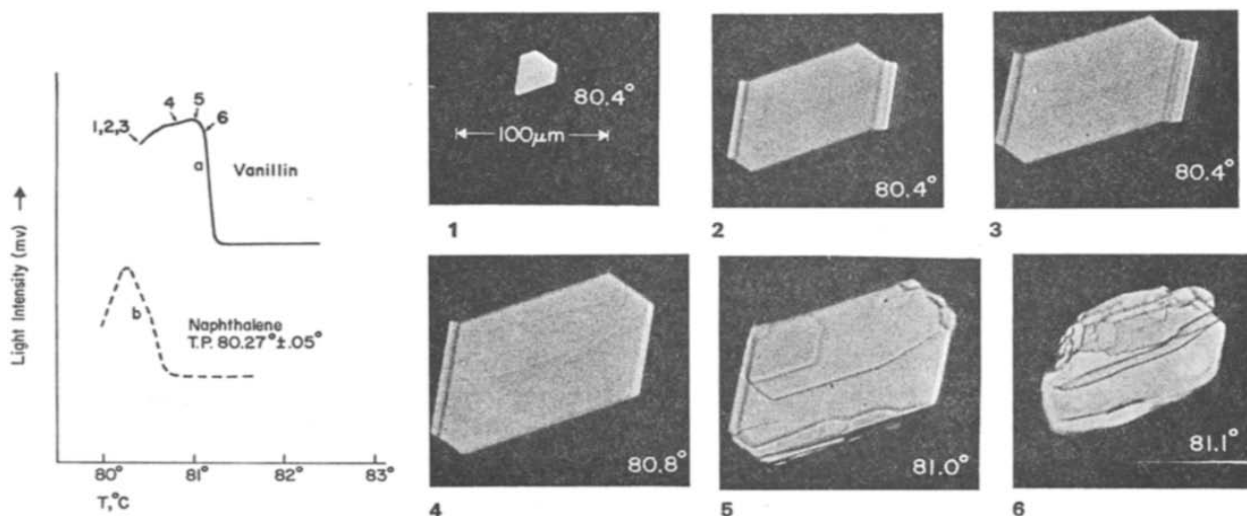


Fig. 15. The microscope hot stage melting at 0.2°/min of a single growing crystal of vanillin (curve a) simultaneously recorded and photographed. The dark area in the photomicrographs is liquid vanillin melt as it appears between crossed polarizing filters. Curve b shows a calibration recording of the growth and melting of a single crystal of naphthalene in liquid naphthalene (certified triple point 80.27°C). The peak of both curves represents the point of maximum crystal size and thus can be considered to accurately indicate the equilibrium melting point. The crystal masses in both cases are on the order of 0.5 µg.

\*Trademark E. I. Dupont Co.

at room temperature and then remelting it in very small isothermal steps up to about 81°C. Just before the last fragment of crystal melted the temperature was dropped to 80.4°C and held isothermal allowing the single crystal to grow in its own melt as is shown in the first three photomicrographs. The mass of the crystal at this point is about 0.5  $\mu\text{g}$ . The temperature was then increased linearly at 0.2°/min. The recording of light intensity as a function of time and temperature shows increasing growth of the size of the crystal until 81.0°C after which it rapidly decreases in size until it is completely melted at 81.25°C. The photomicrophotographs show initial surface erosion as early as 80.8°C which also appears as a reduction in the rate of increase in light intensity. The isothermal equilibrium melting point can be closely estimated by this technique as between 80.8 and 81.0°C.

A second subsequent calibration test with the same apparatus was made using the same single crystal growth techniques on a sample of a Fisher "Thermetric" standard naphthalene which had a certified triple point<sup>8</sup> of  $80.27 \pm 0.05^\circ\text{C}$ . This test is shown as curve b on Fig. 15. The curve maxima occurred at an indicated value of 80.3°C, showing excellent agreement with the previously certified value.

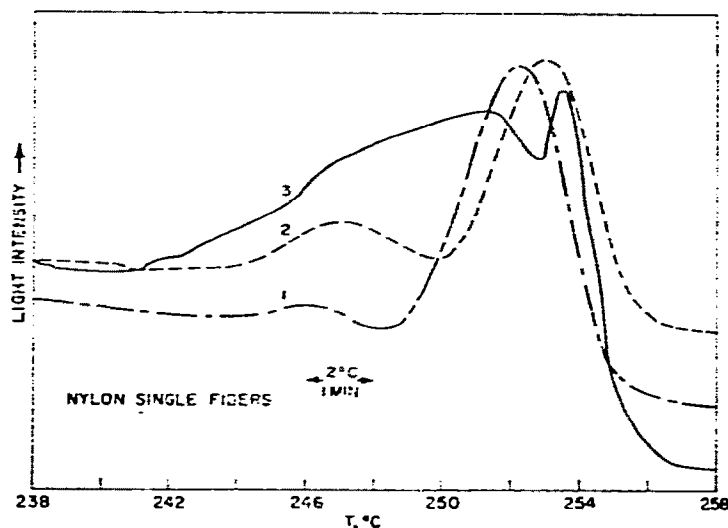


Fig. 16. Microscope hot stage melting of sections of nylon cut from the same length of fiber. Birefringence completely disappears in all three cases at  $257 \pm 0.2^\circ\text{C}$ . Bright color changes which show up as peaks and valleys on the recording, are similar to those seen in the drawn Mylar (Fig. 14).

Fig. 16 shows three melting curves of single fibers of nylon cut from the same length of fiber. Variations in the signal prior to melting are due to changes in the birefringence color between blue, red and yellow. Polymer melting-point determinations, in particular, lend themselves to the microscope rather than capillary technique since it is very difficult to load fibers or film into a small capillary, whereas mounting even a single fiber on a microscope slide is a simple operation. The reverse phenomena or rates of crystallization of polymers at various isothermal temperatures measured by a microscope, photometer, hot stage combination has been described in detail by Magill<sup>13</sup> in 1961.

Visual observation, made possible by the microscope, is very useful in many types of measurements when performed by an experienced observer. Photometric recording, however, is a useful supplement in that it may provide a continuous dynamic record of data as a function of temperature, which is useful in many measurements and specially useful in rapidly communicating observations to others<sup>14, 15</sup>. In the case of polymer melting-point determinations, photometric recording has an advantage over visual observation in that melting ranges are relatively wide and, therefore, tedious to watch at slow rates of heating. In the case of low crystallinity materials such as low-density polyethylene, the gradual change in birefringence contrast is very subtle and may be partially missed by the human eye (Fig. 17). Time-lapse cinemicrography and still photomicrography are additional techniques of recording thermal microscopy data when the additional details recorded warrant the time and effort.

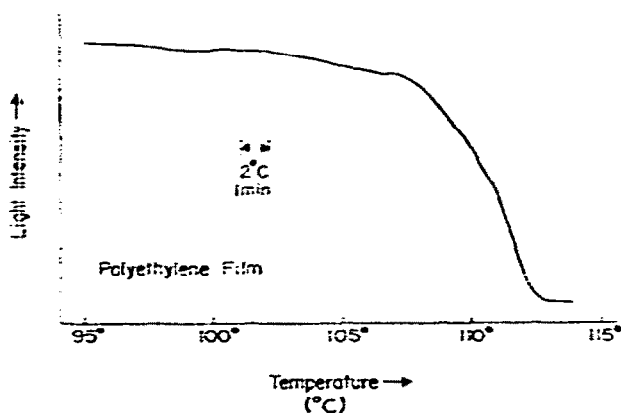


Fig. 17. Microscope hot stage melting of polyethylene film. Birefringence appears as a dull grey with slowly decreasing intensity until melting is complete at 112.5°C.

#### *Relationship of photometric measurements to DTA*

The technique of differential thermal analysis is presently widely applied to both calorimetric measurements (heats of fusion, transformation, *etc.*) as well as thermometric measurements (melting points, solid state transformation temperatures, *etc.*).

The measured thermal effects in differential thermal analysis have been shown to be proportional to the square root of the heating rate, as well as a direct function of the size of the sample. The resolving power of a given DTA apparatus, however, is an inverse function of the size of the sample and heating rate<sup>16, 17, 18</sup>. Very small samples at very slow heating rates often do not produce a measurable signal. Low energy processes at isothermal temperatures cannot be measured at all. Optical properties, on the other hand, are completely independent of heating rate. Transformations, fusion phenomena, decompositions, may be observed at constant or linearly changing temperature over a period of hours, if desired, with no loss in measurement ability. Small mass samples rather than reducing the measured effect, as is the case

in DTA, actually enhance clarity of observation. The size sample required for thermal microscopy at standard  $100\times$  magnification ranges from a few nanograms to a fraction of a milligram.

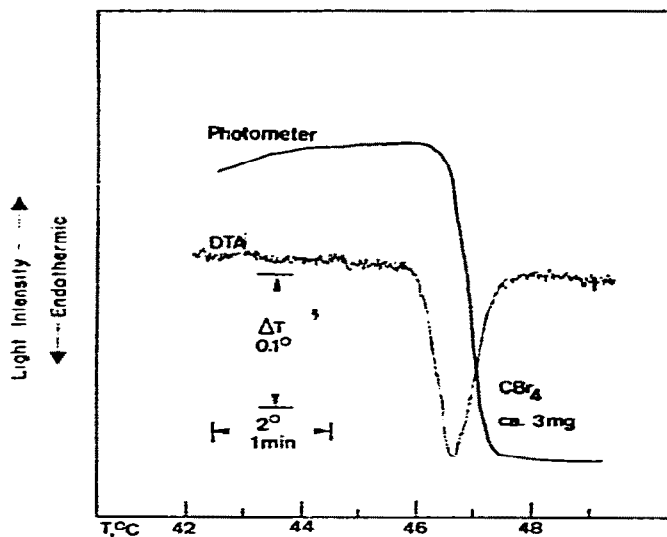


Fig. 18. Simultaneous DTA and photometric measurements of the monoclinic, octahedral transformation of tetrabromomethane. The octahedral form is isotropic, whereas the monoclinic form is brightly colored, making the transformation easy to follow both visually and photometrically.

Tests have shown that visual phenomena associated with fusion and with transformations occur over the same temperature range as the enthalpic phenomena

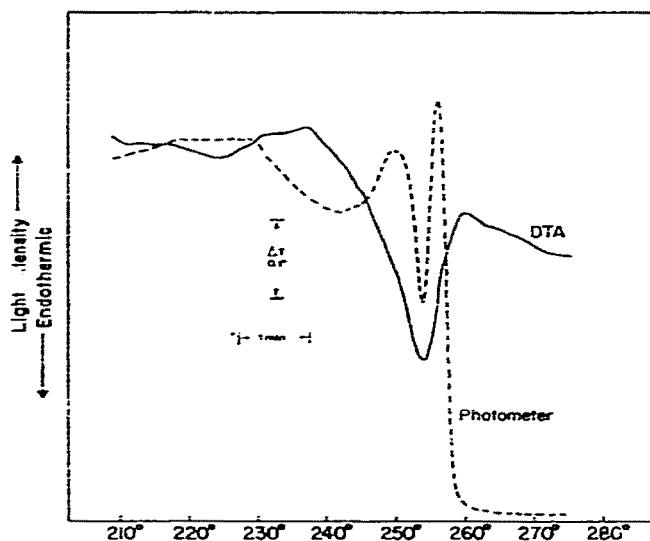


Fig. 19. DTA and photometric measurements of Mylar film, showing the relationship between change in birefringence and various points on the DTA curve. The DTA peak corresponds to the point where the polymer first "wets" the microscope slide cover glass. Birefringence persists, however, until the end of the DTA peak at 259°C.

measured by DTA. Fig. 8 shows the monoclinic to octahedral transformation of tetrabromomethane, measured simultaneously by a microscope photometer and by a DTA thermocouple mounted on the sample carrier slide<sup>16</sup>. The higher-temperature octahedral form is isotropic, whereas the monoclinic form is brightly colored between crossed polarizers. The change in crystal form is very easy to follow with the photometer. Fig. 19 shows the simultaneous photometer-DTA measurement of a thin film of Mylar, again between crossed polarizers. The photometer measures the change in birefringence order as the sample changes from green to red to green and finally to orange, white, gray then black, during the final photometer peak. The sample first appears to "wet" the cover glass at about 255°C. At 259°C no further birefringence persists, indicating the complete change from crystalline to amorphous material. The DTA curve shows the same effect. Barrall and Gallegos described this same correspondence between DTA and microscopy although measurements were made on separate instruments rather than simultaneously<sup>19,20</sup>.

#### REFERENCES

- 1 J. THIELE, *Chem. Ber.*, 40 (1907) 966.
- 2 L. KOFLER and H. HILBECK, *Mikrochemie*, 9 (1931) 38.
- 3 W. C. McCRONE, *Fusion Methods in Chemical Microscopy*, Interscience, New York, N. Y., 1957.
- 4 C. PLATO and A. R. GLASGOW, JR., *Anal. Chem.*, 41 (1969) 330.
- 5 C. R. WITSCHONKE, *Anal. Chem.*, 26 (1954) 562.
- 6 A. STEYERMARK, *Quantitative Organic Microanalysis*, 2nd ed., Academic Press, New York, N. Y., 1961, pp. 528.
- 7 H. G. WIEDEMANN and A. VAN TETS, *Z. Anal. Chem.*, 233 (1968) 161.
- 8 V. G. COLARUSSO and M. A. SEMON, *Anal. Chem.*, 40 (1968) 1521.
- 9 F. W. SCHWAB and E. WICHERS, *J. Res. Nat. Bur. Stand.*, 34 (1945) 333.
- 10 Clairex Corporation, *Photoconductive Cell Design Manual*, New York, N. Y., 1966.
- 11 H. JUCKER and H. SUTER, *Fortschr. Chem. Forsch.*, 11 (1969) 430.
- 12 A. WEISSBERGER, *Physical Methods of Organic Chemistry*, Vol. 1, Interscience, New York, N. Y., 1945, pp. 1, 2.
- 13 J. H. MAGILL, *Polymer*, 2 (1961) 221.
- 14 H. P. VAUGHAN, *Microscope*, 17 (1969) 71.
- 15 A. K. KOLB, C. L. LEE, and R. M. TRAIL, *Anal. Chem.*, 39 (1967) 1206.
- 16 A. VAN TETS and H. G. WIEDEMANN, in R. F. SCHWENKER and P. D. GARN (Eds.), *Thermal Analysis*, Vol I, Academic Press, New York, N. Y., 1969, p. 121.
- 17 A. P. GRAY, in R. S. PORTER and J. F. JOHNSON (Eds.), *Analytical Calorimetry*, Plenum, New York, N. Y., 1968, p. 209.
- 18 W. H. KING, JR., A. F. FINDEIS, AND C. T. CAMILLI, see Ref. 17, p. 261.
- 19 E. M. BARRALLI AND E. J. GALLEGOS, *J. Polymer Sci. 2A*, 5 (1967) 113.
- 20 E. M. BARRALLI, J. F. JOHNSON AND R. S. PORTER, *Appl. Polym. Symp.*, 8 (1969) 191.